IOP Publishing Environ. Res. Lett. 19 (2024) 024020 https://doi.org/10.1088/1748-9326/ad1d3b

ENVIRONMENTAL RESEARCH
LETTERS

LETTER

Observations reveal onshore acceleration and offshore deceleration of the Kuroshio Current in the East China Sea over the past three decades

Haihong Guo[1,2,3], **Jinzhuo Cai**[2,3], **Haiyuan Yang**[1,2,*] **and Zhaohui Chen**[1,2]

[1] Laoshan Laboratory, Qingdao, People's Republic of China
[2] Frontier Science Center for Deep Ocean Multispheres and Earth System (FDOMES)/Academy of the Future Ocean and Physical Oceanography Laboratory, Ocean University of China, Qingdao, People's Republic of China
[3] These authors contributed equally to this article.
[*] Author to whom any correspondence should be addressed.

E-mail: yanghaiyuan@ouc.edu.cn

Keywords: Kuroshio Current, East China Sea, onshore acceleration, offshore deceleration, enhanced stratification, weakened wind

Supplementary material for this article is available online

OPEN ACCESS

RECEIVED
15 November 2023

REVISED
5 January 2024

ACCEPTED FOR PUBLICATION
10 January 2024

PUBLISHED
25 January 2024

Abstract

The Kuroshio Current (KC) in the East China Sea is one of the most prominent components of the ocean circulation system in the North Pacific. The onshore intensification of the KC is found to drive nutrient-rich upwelling in the shelf regions, induce anomalous warming that leads to coastal marine heatwaves, and reduce the ability of the oceans to absorb anthropogenic carbon dioxide. Based on altimeter and *in situ* observations, we find an onshore acceleration and offshore deceleration of the KC over the past three decades. This intensification is characterized by a spatial mean onshore acceleration (offshore deceleration) of 0.39 (−0.63) cm s^{-1} per decade. This phenomenon can be attributed to changes in wind stress curl (WSC) and oceanic stratification over the subtropical North Pacific. The weakened WSC decreases the vertical extent of the KC by reducing its transport and contributes to the offshore deceleration, whereas the enhanced stratification drives the uplift of the KC and contributes to the onshore acceleration. Our findings underscore the importance of establishing and maintaining a long-term monitoring network for the zonal variations of the KC in the future to obtain a comprehensive understanding of the associated impacts.

1. Introduction

The Kuroshio Current (KC) is one of the most prominent components of the circulation system in the North Pacific Ocean, serving as an efficient conveyor of mass and energy between the tropical and mid-latitude regions (Imawaki *et al* 2013, Hu *et al* 2015, Storer *et al* 2022). Originating from the bifurcation of the North Equatorial Current (Nitani 1972, Qiu and Lukas 1996), it flows northward along the eastern coast of the Philippines Islands and Taiwan Island. To the northeast of Taiwan, the KC flows over the Ilan Ridge and enters the East China Sea (ECS), where it meanders along the continental slopes of the ECS with a stable volume transport of approximately 24 Sv (1 Sv = 10^6 m^3 s^{-1}; Andres *et al* 2008a, Liu *et al* 2021b). At 30°N, the KC exits the ECS through the Tokara Strait (Imawaki *et al* 2013). Using both *in situ* and satellite altimeter observations, the transport and variabilities of the KC in the ECS have been well investigated (Andres *et al* 2008b, Zhu *et al* 2017). In addition to these studies, it is imperative to elucidate the zonal variations of KC, particularly focusing on the long-term changes and their underlying mechanisms.

Zonal variations of the KC could have substantial impacts on continental shelves and coastal areas in the ECS (Yang *et al* 2018). For example, an anomalous shoreward KC interacts with bottom topography and drives intense nutrient-rich upwelling on continental shelves (Yang *et al* 2011, Cui *et al* 2021, Sun *et al* 2022), which fertilizes coastal areas such

as the Zhoushan fishing ground (Lin *et al* 2019). Additionally, an anomalous onshore movement of the KC could result in significant warming of the Pacific Asian marginal seas, especially the continental shelf of the ECS, contributing to the formation of intense marine heatwaves (Lee *et al* 2023, Wang *et al* 2023). For instance, the rapid warming of the East Asian marginal seas is attributed to the Kuroshio intrusion (Wang and Wu 2022). Besides, anomalously high temperatures reduce the solubility of carbon dioxide, limiting the oceans' capacity to absorb anthropogenic carbon dioxide from the atmosphere (Cai *et al* 2006, Wu *et al* 2012). Furthermore, this warming could destabilize or even lead to the release of a large amount of methane hydrate stored beneath the seafloor of shelf regions in the ECS (Guan *et al* 2022), exacerbating the warming of the surrounding climate system and increasing the risk of geological disasters.

Based on temperature observations, reanalysis, and model products, the subtropical gyre in the North Pacific has been observed to undergo a poleward intensification during the 20th century (Wu *et al* 2012, Yang *et al* 2020), featuring enhanced warming in the Kuroshio Extension regions (Wu *et al* 2012). Many reports have focused on the zonal variations of the KC axis, extensively examining its high-frequency variations (Kawabe 1995, Nakamura *et al* 2003, Liu *et al* 2019). However, due to the limited duration of ocean current observations and the coarse resolution of numerical models, how the long-term zonal characteristics of the KC in the ECS might change, which is crucial for projecting changes in the ECS and surrounding areas, remains unknown. Here, using high-resolution observations and available reanalysis products, we identify an onshore acceleration and offshore deceleration of the KC in the ECS over the past three decades.

2. Data and method

To explore the zonal variations of the KC, we initially utilize surface geostrophic velocity derived from the Ssalto/Duacs altimeter products (supporting information text S1). These products offer high-resolution (0.25°) global coverage of ocean surface topography and currents, allowing us to observe narrow currents. Commencing from October 1992 and continuing to the present, this data provides a valuable tool for studying the trends of surface velocity. In this study, we utilize monthly mean data to calculate surface velocity trends from 1993 to 2021 (Ducet *et al* 2000). In addition, we utilize *in situ* temperature and salinity data from the Japan Meteorological Agency (JMA; available at www.data.jma.go.jp/) to calculate geostrophic velocity across the PN section (dashed line connecting 29° N, 126° E and 27° N, 128.5° E; figure 1(a)). The product offers over 90 cruises with more than 3000 vertical profiles of oceanic temperature and salinity on isobaric surface along PN from 1997 to 2021, allowing us to calculate geostrophic velocity from bottom of the ocean to the surface (supporting information text S2).

Given that the western boundary current is primarily influenced by wind stress curl (WSC) and oceanic stratification, we analyze the corresponding variations in wind and stratification using observational and reanalysis datasets. We employ wind stress data sourced from three datasets: the European Centre for Medium-Range Weather Forecasts (ECMWF) Reanalysis Version 5 (ERA5; Hersbach *et al* 2023), the Cross-Calibrated Multi-Platform (CCMP; Mears *et al* 2022), and the National Centers for Environmental Prediction Reanalysis 1 (NCEP1; Kalnay *et al* 1996). Meanwhile, to examine changes in stratification, we utilize temperature and salinity data derived from the Estimating the Circulation and Climate of the Ocean 2 (ECCO2; Menemenlis *et al* 2005), the Ocean Reanalysis System 5 (ORAS5; Copernicus Climate Change Service) from the ECMWF, and the NCEP Global Ocean Data Assimilation System (GODAS; Behringer *et al* 1998). Oceanic stratification is calculated using the Gibbs Seawater Oceanographic Toolbox, which utilizes temperature and salinity data (McDougall and Barker 2011). All the datasets are uniformly remapped to a $1° \times 1$ grid (120° E–120° W, 15–30° N), with monthly means spanning from 1993 to 2021, aligning with the altimeter data. Detailed information about these datasets can be found in supporting information text S3. To mitigate bias resulting from variations in different datasets, we calculate the ensemble mean for each variable.

Furthermore, to investigate the mechanisms of wind forcing and oceanic stratification on the zonal variations of the KC, we conduct a series of idealized numerical experiments using the Massachusetts Institute of Technology general circulation model (MITgcm; Marshall *et al* 1997; for detailed model configurations, please refer to supporting information text S4).

To compute the zonal variation of the KC, it is necessary to first define the current axis. The axis of the KC is determined by the 1.1 m contour line of mean sea surface height observed from satellites during 1993–2021 (black lines in figure 1(a)). The spatial mean trend of surface velocity on both sides of the axis is determined by averaging within a 1° band (enclosed by the green line in figure 1(a)) on the western and eastern sides of the axis. The onshore/offshore transport of the KC along the PN line is calculated within a 100 km band on both flanks. The axis of the KC in the MITgcm model is defined by the location of the maximum transport of the modeled KC.

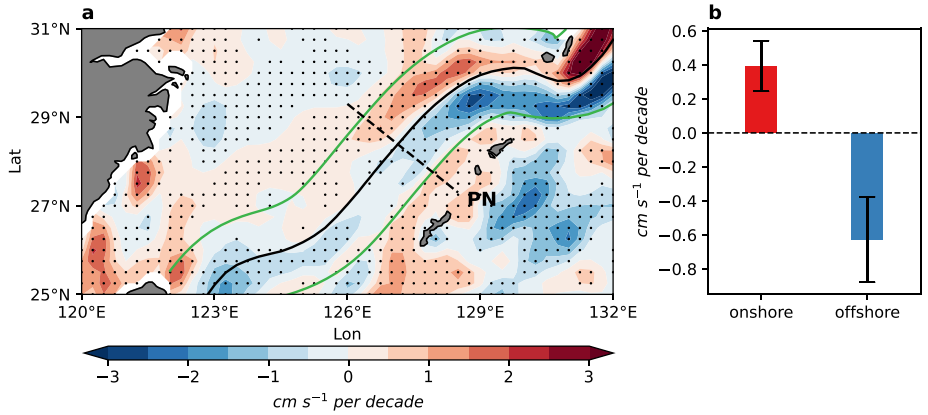

Figure 1. (a), Linear trends of surface geostrophic velocity (cm s^{-1} per decade) in the KC region during 1993–2021. The black dots represent the trends that are statistically significant above the 90% confidence level estimated by Student's T-test. The solid black lines are the KC axis defined by the 1.1 m contours of the time-mean sea surface height from satellites (Wang and Tang 2022). The dashed black line represents the PN section. The green lines enclose the 1° band on both sides of the axis. (b), Trends averaged within 1° band on the onshore and offshore flanks of the KC axis. The error bars indicate the 90% confidence interval level estimated by Student's T-test.

3. Observed zonal variations of the KC

The surface velocity trends of the KC display opposing signs with respect to the KC axis (figure 1(a)), marked by acceleration on the onshore side and deceleration on the offshore side of its axis, respectively. This antisymmetric pattern starts from the dipolar northwest of Taiwan at 25° N, where the upstream KC interacts with the Ilan Ridge and subsequently enters the ECS (figure 1(a)). Although the magnitude of trends within 26° N–28° N is relatively small, the opposing pattern remains conspicuous. Between the PN section (straight line connecting 29° N, 126° E and 27° N, 128.5° E; dashed line in figure 1(a)) and Tokara Strait, the magnitude of trends becomes strong again.

To further validate the zonal variations of KC, we calculate the spatial mean velocity trends on the two flanks of the KC axis (regions between green lines and the KC axis in figure 1(a)). The mean magnitudes of the onshore acceleration (red bar) and offshore deceleration (blue bar) are 0.39 ± 0.18 and -0.63 ± 0.30 cm s^{-1} per decade, respectively (figure 1(b)). Quantitatively, the trend indicates a velocity increase by 3.2% on the onshore flank, and a decrease by 4.6% on the offshore flank in the past three decades, suggesting that the KC tends to travel more along the onshore side of its axis, bringing warmer and saltier KC water onto the ECS shelf.

Besides altimeter observations, the onshore strengthening and offshore weakening of the KC are also captured by *in situ* observations along the PN section (dashed lines in figure 1(a)). The KC flows across the PN line in the central ECS and maintains a time-mean volume transport of 23.3 Sv, consistent with previous studies (Imawaki *et al* 2013). Figure 2(a) reveals that the change of the KC is not confined to the surface. The cross-section velocities in the upper 800 m along the PN section exhibit a similar antisymmetric pattern as the surface velocity, with a maximum positive (negative) value located at the locations of $x = 100$ km ($x = 170$ km). Because the ocean depth increases from the onshore side of the KC to the offshore side, the transport trend of KC on the offshore side exhibits a relatively larger amplitude (figure 2(b)). Quantitatively, the transport on the onshore side of the KC exhibits an increase trend of 0.40 ± 0.33 Sv per decade, whereas the offshore transport displays a decrease trend of -0.73 ± 0.72 Sv per decade. In addition, it is noted that the vertical extent of the positive velocity trend is relatively shallower than that of the negative trend, suggesting a shallower KC over the past three decades.

4. Associated changes in wind forcing and oceanic stratification

Two primary processes that could contribute to changes in the KC are the wind field (Stommel 1948, Sen Gupta *et al* 2021) and oceanic stratification (Pedlosky 1987, Peng *et al* 2022). The former directly determines the intensity of the KC, whereas the latter influences its vertical extent. For instance, the weakening of the Kuroshio from 1993 to 2013 can be attributed to the weakened westerlies and cyclonic trends of basin-scale (WSC; Wang *et al* 2016). The enhanced vertical stratification in a warming climate will intensify the upper subtropical gyres by shoaling these systems (Peng *et al* 2022). To explore the role of wind and stratification in governing the zonal variations of the KC, we proceed to evaluate their changes by analyzing observational data and reanalysis products.

According to the wind-driven circulation theory, the KC is primarily driven by the presence of negative

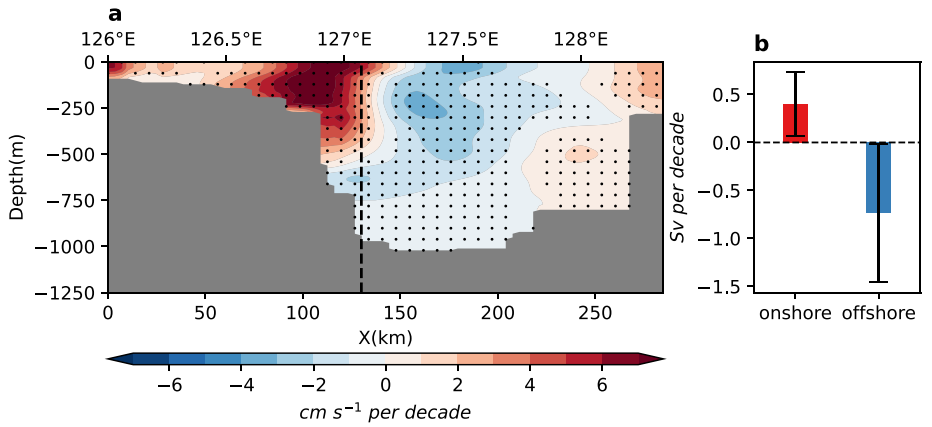

Figure 2. (a) Linear trend of geostrophic velocity (cm s^{-1} per decade) across the PN line (dashed black line in figure 1(a)) during 1997–2021, based on *in situ* observations from JMA. Positive (negative) values indicate the acceleration (deceleration) of the current. The black dots indicate that the trend is statistically significant above the 90% confidence level estimated by Student's T-test. The vertical dashed line indicates the axis of KC. (b) Magnitude of the transport trends on the onshore and offshore flanks of the KC. The error bars indicate the 90% confidence interval level estimated by Student's T-test.

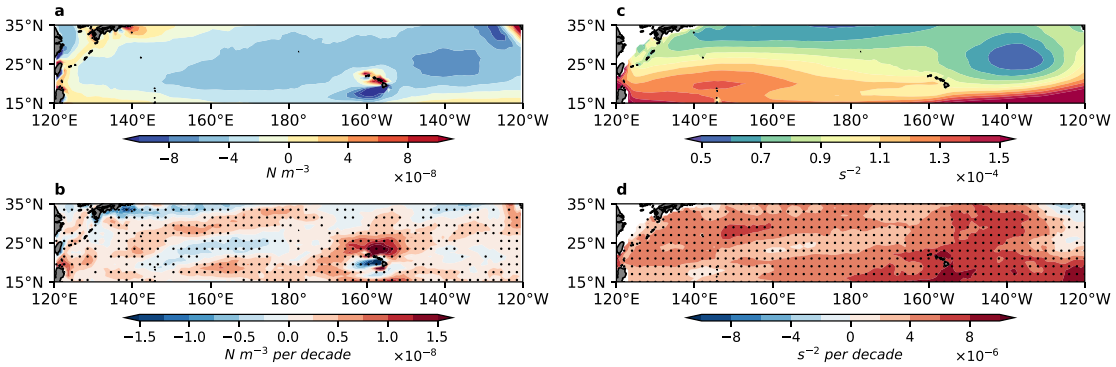

Figure 3. (a), (b) Time-mean WSC (a) and linear trend (b) for the period of 1993–2021, based on ensemble mean of ERA5, CCMP, and NCEP1. (c), (d) Time-mean oceanic stratification averaged at depths between 0 and 200 m (c) and linear trend (d) during 1993–2021, based on ensemble mean of ECCO2, ORAS5, and GODAS datasets. The black dots in (b) and (d) denote that the trend is statistically significant above the 90% confidence level estimated by Student's T-test.

WSC over the subtropical North Pacific (figure 3(a); Stommel 1948, Pedlosky 1987), with an approximate spatial mean of 3.6×10^{-8} N m^{-3}. These negative WSCs have exhibited a positive trend from 1993 to 2021, indicating a weakening in wind forcing (figure 3(b)). The difference in spatial mean WBC between 2017–2021 (the last 5 years of the data) and 1993–1997 (the first 5 years of the data) ranges from 2.8×10^{-9} N m^{-3}–4.5×10^{-9} N m^{-3} in different datasets (supporting information table 1), consistent with the observed weakening of westerlies over the North Pacific (Wang *et al* 2016).

Regarding oceanic stratification, the vertical mean stratification over the upper 200 meters reveals a latitude-dependent pattern with larger values in the subtropical ocean than in high-latitude regions (figure 3(c)). Over the past three decades, there has been a synchronous enhancement of oceanic stratification in the subtropical North Pacific (figure 3(d)). The difference in spatial mean stratification between 2017–2021 and 1993–1997 ranges from 8.0×10^{-6} s^{-2} to 11.0×10^{-6} s^{-2} in different datasets (supporting information table 1). This enhanced stratification aligns with rising sea surface temperatures (Capotondi *et al* 2012) and tends to trap more energy in the upper ocean. Overall, a weakening wind stress curl and an intensifying oceanic stratification are detected in the North Pacific over the past three decades.

5. Mechanisms of wind forcing and oceanic stratification

In this section, we delve into the underlying mechanisms of wind forcing and oceanic stratification using an idealized MITgcm model. The model domain includes a shallow coastal shelf and a flat deep ocean linked by a continental slope (supporting information figure S1(a)). Since the intensified stratification in the subtropical North Pacific is primarily

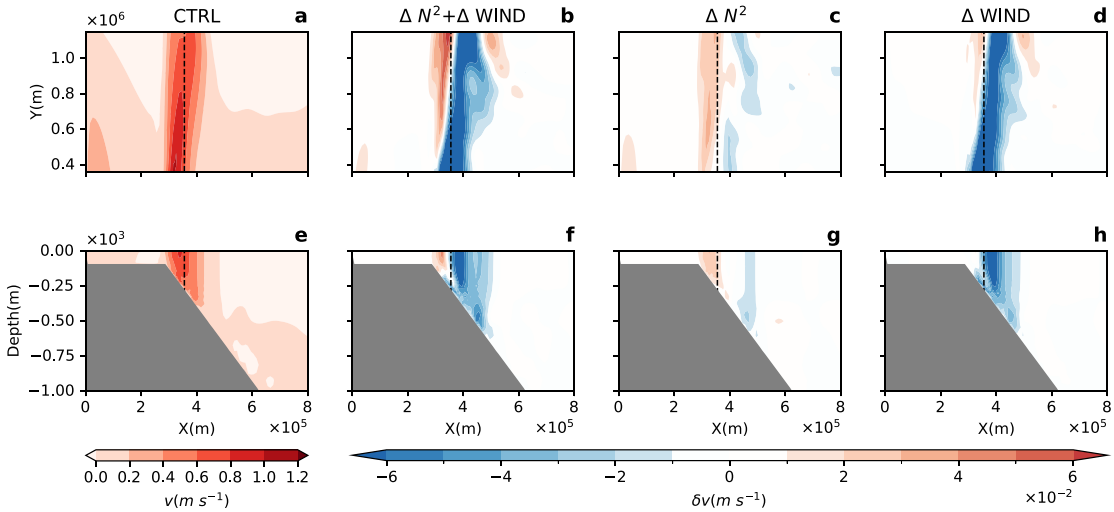

Figure 4. (a), Horizontal distribution of the surface meridional velocities in the western boundary region of the CTRL run. (b)–(d), Meridional velocity changes in $\triangle N^2+\triangle$WIND run (b), $\triangle N^2$ run (c), and $\triangle$WIND run (d) relative to the CTRL run. The dashed line denotes the axis of the Kuroshio. (e)–(h), same as a–d but for the vertical section of the meridional velocities. The vertical section is located at the meridional center of the model domain (supporting information figure S1(a)).

determined by temperature variations (Li *et al* 2020), the ocean salinity is maintained constant at 35 g kg^{-1}, while the vertical temperature profile is averaged over the subtropical basin. Hence, the stratification exclusively follows the changes in temperature (supporting information figure S1(b)). The wind forcing is represented by an idealized cosine zonal wind stress, featuring easterly trade winds in low latitudes and westerly winds in mid-latitudes (supporting information figure S1(c)).

The numerical experiments consist of four runs: a simulation driven by climatological mean wind forcing and oceanic temperature data sourced from observational and reanalysis datasets (referred to as CTRL run), a simulation accounting for changes in both wind forcing and stratification ($\triangle N^2+\triangle$WIND run), as well as two simulations separately considering changes in stratification ($\triangle N^2$ run; N^2 indicates buoyancy frequency) and wind forcing ($\triangle$WIND run), respectively. In the latter three runs, changes in stratification and wind forcing are based on the difference between 2017–2021 and 1993–1997 in the ensemble mean of available datasets (supporting information text S3; figure 3). Consequently, these simulations enable us to evaluate the behavior of the KC and the relative importance of changes in stratification and wind forcing.

Figure 4 illustrates the modeled velocity in the CTRL run and its anomalies for the diagnostic runs. The KC flows along the continental slope, with a maximum surface velocity of approximately 1.0 m s^{-1} (figure 4(a)), consistent with *in situ* observations (Imawaki *et al* 2013). In response to the changes in stratification and wind (figure 4(b)), the poleward velocity anomalies exhibit a dipole pattern, characterized by acceleration on the onshore side and deceleration on the offshore side of the mean current axis, which is consistent with satellite observations. In the $\triangle N^2$ run, enhanced stratification results in a similar onshore velocity change (figure 4(c)), suggesting that the onshore intensification of KC is mainly induced by enhanced stratification. By comparison, significant deceleration is found on the offshore flank in the $\triangle$WIND run (figure 4(d)), indicating that weakened wind primarily leads to an offshore and overall weakening of the current. In addition to surface velocity, the evolution of the KC can also be revealed by comparing the meridional velocity distribution along the zonal section at the center of the models (figures 4(e)–(h)), where the increased (decreased) velocity on the onshore (offshore) flank is also prominent.

As discussed in section 2, the onshore acceleration and offshore deceleration of the KC suggest that a larger volume of water tends to flow along the shallower shelf regions, indicating a vertical compression of the KC. According to wind-driven circulation theory, we can estimate the vertical scale of the circulation system through vorticity balance (supporting information text S5, Young and Rhines 1982, Guo and Spall 2021, Guo *et al* 2022), which gives a vertical scale of the KC as

$$D = \left(\frac{f^2|\mathrm{curl}(\boldsymbol{\tau})|}{N^2\beta^2\rho_0}\right)^{1/3}, \quad (1)$$

where f denotes the Coriolis parameter, τ stands for the wind stress, N denotes the buoyancy frequency, β represents the meridional variation of the Coriolis parameter, and ρ_0 is seawater density. This method has been successfully applied in previous studies to elucidate the vertical scale of wind-driven circulation

near continental or island boundaries (Guo and Spall 2021, Guo *et al* 2022).

According to equation (1), both weakened wind stress curl ($|\mathrm{curl}(\boldsymbol{\tau})|$) and enhanced stratification (N^2) could result in a smaller vertical scale (D) of the KC. Dynamically, the weakened wind stress curl leads to a reduced input of vorticity into the ocean interior, resulting in a low-level vorticity balance in the western boundary region. Therefore, the wind stress curl plays a crucial role in determining the background strength of the vorticity balance in the KC region (equation (E2) in supporting information text S5). In comparison, increased stratification does not alter the overall strength of the vorticity balance but amplifies vorticity stretching, thus leading to a reduction in vertical scale. The vertically compressed KC tends to shift more westward toward shallower areas. As a result, the proportion of KC water on the onshore side increases, while it decreases on the offshore side, leading to an onshore intensified KC.

By substituting the wind stress curl and temperature profile from the CTRL run into equation (1), we obtain the reference value of D, which is 232.1 m. Over the past 30 years, enhanced stratification and weakened WSC over the North Pacific lead to changes in D of 11.8 m. By considering the effect of stratification and wind independently, we find that the enhanced stratification is responsible for ∼40% changes in D (−4.7 m), while the weakened WSC accounts for ∼60% (−7.8 m).

To validate our results, we further examine the sensitivity of our results to the slope. The bottom slope from the PN section to the Tokara Strait is steeper than the slope from northeastern Taiwan to the PN section. To explore the relationship between the onshore intensification of the KC and bottom topography, we conduct a series of new experiments. In these experiments, the topographic slope becomes gentler at higher latitudes (supporting information figure S2). The other parameters remain consistent with both the CTRL run and the $\triangle N^2+\triangle$WIND run. It is intriguing to note that the onshore intensification feature is not as pronounced upstream where the topographic slope is steeper. However, in the downstream region with a gentler slope, the onshore intensification becomes more pronounced. This is because, in regions with a steeper slope, the ratio of the zonal shift of the KC to its vertical compression is small, resulting in a less significant zonal shift for the same vertical compression. Hence, the strength of the onshore intensified KC significantly relies on the slope of the bottom topography. Nevertheless, the asymmetry in velocity anomalies is distinct and aligns consistently with our theory.

Therefore, both weakened WSC and enhanced stratification are responsible for a shallower and more shoreward KC. According to the Sverdrup balance theory, the total transport of a western boundary current is determined by the ocean interior wind stress curl and Coriolis parameters (f and β; Sverdrup 1947). Thus, the total transport of the KC is unaffected by enhanced stratification but relies on wind variations, even though the variabilities of the KC depend on global warming (Chen *et al* 2019, Sasaki and Umeda 2021, Liu *et al* 2021a). Dynamically, the weakened WSC decreases the vertical extent of KC by reducing its transport and contributes more to the offshore deacceleration, whereas the enhanced stratification drives the uplift of KC and contributes more to the onshore acceleration. The vertical structure of the KC is determined by the large-scale stratification and wind stress curl across the entire subtropical region, considering the KC's origin from the interior southward Sverdrup transport, representing a remote effect. This is distinct from the enhanced stratification along the current stream resulting from an enhanced KC, which only alters the local hydrological properties.

The onshore intensification of the KC resembles the reported poleward shift of this current (Yang *et al* 2020), both pointing to an outward expansion of the KC. However, the underlying mechanisms governing shoreward and poleward intensifications of the KC are different. The poleward intensification observed in the KC extension region results from the poleward intensification of the subtropical westerlies and the expansion of the Hadley Cell (Sen Gupta *et al* 2021). Consequently, the poleward shift of the KC is significantly more pronounced than the onshore intensification of the KC (Yang *et al* 2020). In contrast, the onshore intensification of the KC is primarily linked to the vertical compression of the current due to enhanced stratification and weakened wind stress curl.

6. Summary and implications

The observed onshore acceleration and offshore deceleration of the KC over the past three decades are attributed to both the weakened WCS and the enhanced stratification over the subtropical North Pacific. They induce transport reduction and uplift of KC, leading to the opposite changes on the onshore and offshore flanks in observation. The intensity of changes on both sides of the KC axis depends on the slope of the bottom topography, exhibiting a more pronounced magnitude in steeper regions. It is important to note that variations in stratification and wind may also encompass some internal variabilities, such as the Pacific Decadal Oscillation (PDO), which could significantly modulate the KC (Andres *et al* 2009, Wei *et al* 2013). The PDO demonstrates an inverse relationship with onshore intensification, with a correlation of −0.77 (supporting information figure S3). This correlation aligns with our proposed theory. During the positive phase of

the PDO, the Northwestern Pacific exhibits a negative sea surface temperature (Alexander 2010), signifying weakened stratification. Simultaneously, there is a negative anomaly in WSC over the subtropical North Pacific, indicating strengthened WSCs (Wu *et al* 2019), consistent with the offshore-intensified KC.

Our discovery in this study is an important finding with profound implications. The shoreward movement of the KC interacts with the topography, driving nutrient-rich upwelling on continental shelves, and enriching coastal areas such as the Zhoushan fishing ground (Lin *et al* 2019). The rapid surface warming induced by the acceleration of the Kuroshio on the onshore side (Sasaki and Umeda 2021, Wang and Wu 2022) could potentially lead to more intense marine heatwaves (Oliver *et al* 2021). The onshore intensification of the KC results in a more rapid increase in ocean heat content on the onshore side compared to the offshore side (supporting information text S6). Further, as a consequence of the enhanced warming, a reduced ocean ability to absorb carbon dioxide (Cai *et al* 2006) and a destabilized methane hydrate (Guan *et al* 2022), is likely to occur in the coastal and continental shelf regions in the ECS.

The observed trend of the onshore-intensified KC includes some internal variabilities, requiring a long-term monitoring network for investigating these variations. Moreover, the significant implications of the onshore-intensified KC also require more attention. Therefore, our findings underscore the pressing need for a comprehensive assessment of the impacts associated with zonal variations of the KC in the future.

Data availability statements

The two-satellite merged sea level gridded data from satellite observations can be accessed at https://doi.org/10.24381/cds.4c328c78. Shipboard observed *in-situ* temperature and salinity data are available from the JMA (www.data.jma.go.jp/). Time-mean temperature profiles can be obtained from WOA18 (www.ncei.noaa.gov/archive/accession/NCEI-WOA18). Monthly wind vectors are accessible on the websites of ERA5 (https://doi.org/10.24381/cds.f17050d7), CCMP (https://doi.org/10.56236/RSS-uv1m30), and NCEP1 (https://psl.noaa.gov/data/gridded/data.ncep.reanalysis.html). Monthly temperature and salinity data are accessible on the website of ECCO2 (https://ecco.jpl.nasa.gov/drive/files/ECCO2/cube92_latlon_quart_90S90N), ORAS5 (https://doi.org/10.24381/cds.67e8eeb7), and GODAS (https://psl.noaa.gov/data/gridded/data.godas.html). The MITgcm model package can be obtained from http://mitgcm.org/.

All data that support the findings of this study are included within the article (and any supplementary files).

Acknowledgments

This work was supported by the National Natural Science Foundation of China (42176006, 42306023 and 42225601), the National Key Research and Development Program of China (2022YFC3104801 and 2022YFC3104205). H G is partly supported by the Shandong Province Postdoctoral Program for Innovative Talents (SDBX2023033). Computation for the work described in this paper was supported by the Marine Big Data Center of Institute for Advanced Ocean Study of Ocean University of China and Laoshan Laboratory.

Ethical statements

This work does not involve live subjects (humans or animals).

Conflict of interest

The authors declare no competing interests.

References

Alexander M 2010 Extratropical air-sea interaction, sea surface temperature variability, and the pacific decadal oscillation *Clim. Dyn.* **189** 123–48

Andres M, Park J H, Wimbush M, Zhu X H, Nakamura H, Kim K and Chang K Il 2009 Manifestation of the Pacific Decadal oscillation in the Kuroshio *Geophys. Res. Lett.* **36** 1–5

Andres M, Park J-H, Wimbush M, Zhu X-H, Chang K-I and Ichikawa H 2008b Study of the Kuroshio/Ryukyu current system based on satellite-altimeter and in situ measurements *J. Oceanogr.* **64** 937–50

Andres M, Wimbush M, Park J H, Chang K I, Lim B H, Watts D R, Ichikawa H and Teague W J 2008a Observations of Kuroshio flow variations in the East China Sea *J. Geophys. Res. Ocean* **113** 1–14

Behringer D W, Ji M and Leetmaa A 1998 An improved coupled model for ENSO prediction and implications for Ocean initialization. Part I: the ocean data assimilation system *Mon. Weather Rev.* **126** 1013–21

Cai W J, Dai M and Wang Y 2006 Air-sea exchange of carbon dioxide in ocean margins: a province-based synthesis *Geophys. Res. Lett.* **33** 2–5

Capotondi A, Alexander M A, Bond N A, Curchitser E N and Scott J D 2012 Enhanced upper ocean stratification with climate change in the CMIP3 models *J. Geophys. Res. Ocean* **117**

Chen C, Wang G, Xie S P and Liu W 2019 Why does global warming weaken the gulf stream but intensify the kuroshio? *J. Clim.* **32** 7437–51

Copernicus Climate Change Service Climate data store 2021 ORAS5 global ocean reanalysis monthly data from 1958 to present *Copernicus Climate Change Service (C3S) Climate Data Store (CDS)* (https://doi.org/10.24381/cds.67e8eeb7) (Accessed 1 May 2023)

Cui X, Yang D, Sun C, Feng X, Gao G, Xu L and Yin B 2021 New insight into the onshore intrusion of the Kuroshio into the East China Sea *J. Geophys. Res. Ocean* **126** 1–19

Ducet N, Le Traon P Y and Reverdin G 2000 Global high-resolution mapping of ocean circulation from TOPEX/Poseidon and ERS-1 and −2 *J. Geophys. Res. Ocean* **105** 19477–98

Guan H, Liu L, Hu Y, Li S, Li N, Sun Z, Wu N and Somerville I 2022 Rising bottom-water temperatures induced methane

release during the middle Holocene in the Okinawa Trough, East China Sea *Chem. Geol.* **590** 120707
Guo H and Spall M A 2021 Topographic influences on the wind-driven exchange between marginal seas and the open ocean *J. Phys. Oceanogr.* **51** 3663–78
Guo H, Spall M A, Pedlosky J and Chen Z 2022 A three-dimensional inertial model for coastal upwelling along Western boundaries *J. Phys. Oceanogr.* **52** 2431–44
Hersbach H *et al* 2023 ERA5 monthly averaged data on single levels from 1940 to present *Copernicus Climate Change Service (C3S) Climate Data Store (CDS)* (https://doi.org/10.24381/cds.f17050d7)
Hu D *et al* 2015 Pacific western boundary currents and their roles in climate *Nature* **522** 299–308
Imawaki S, Bower A S, Beal L and Qiu B 2013 Western boundary currents *International Geophysics* vol 103 (Elsevier Ltd) pp 305–38
Kalnay E *et al* 1996 The NCEP/NCAR 40-year reanalysis project *Bull. Am. Meteorol. Soc.* **77** 437–71
Kawabe M 1995 Variations of current path, velocity, and volume transport of the kuroshio in relation with the large meander *J. Phys. Oceanogr.* **25** 3103–17
Lee S, Park M S, Kwon M, Park Y G, Kim Y H and Choi N 2023 Rapidly changing East Asian Marine heatwaves under a warming climate *J. Geophys. Res. Ocean* **128** 1–20
Li G, Cheng L, Zhu J, Trenberth K E, Mann M E and Abraham J P 2020 Increasing ocean stratification over the past half-century *Nat. Clim. Change* **10** 1116–23
Lin Z, Wang X, Xiu P, Chai F and Wu Q 2019 Boundary phosphate transport of the East China Sea and its influence on biological process *J. Geosci. Environ. Prot.* **07** 79–104
Liu Z J, Nakamura H, Zhu X H, Nishina A, Guo X and Dong M 2019 Tempo-spatial variations of the Kuroshio current in the Tokara Strait based on long-term ferryboat ADCP data *J. Geophys. Res. Ocean* **124** 6030–49
Liu Z J, Zhu X H, Nakamura H, Nishina A, Wang M and Zheng H 2021a Comprehensive observational features for the Kuroshio transport decreasing trend during a recent global warming hiatus *Geophys. Res. Lett.* **48** 1–10
Liu Z, Gan J, Hu J, Wu H, Cai Z and Deng Y 2021b Progress of studies on circulation dynamics in the East China Sea: the Kuroshio exchanges with the shelf currents *Front. Mar. Sci.* **8** 1–17
Marshall J, Hill C, Perelman L and Adcroft A 1997 Hydrostatic, quasi-hydrostatic, and nonhydrostatic ocean modeling *J. Geophys. Res. Ocean* **102** 5733–52
McDougall T J and Barker P M 2011 Getting started with TEOS-10 and the Gibbs Seawater (GSW) oceanographic toolbox *Scor/Iapso WG* **127** 1–28 (available at: www.teos-10.org/software.htm)
Mears C, Lee T, Ricciardulli L, Wang X and Wentz F 2022 Improving the accuracy of the cross-calibrated multi-platform (CCMP) ocean vector winds *Remote Sens.* **14** 4230
Menemenlis D, Fukumori I and Lee T 2005 Using Green's functions to calibrate an ocean general circulation model *Mon. Weather Rev.* **133** 1224–40
Nakamura H, Ichikawa H, Nishina A and Lie H J 2003 Kuroshio path meander between the continental slope and the Tokara Strait in the East China Sea *J. Geophys. Res. Ocean* **108**
Nitani H 1972 Beginning of the Kuroshio *Phys. Asp. Jpn. Curr.* 129–63 (available at: https://cir.nii.ac.jp/crid/1574231875600264832)
Oliver E C J, Benthuysen J A, Darmaraki S, Donat M G, Hobday A J, Holbrook N J, Schlegel R W and Sen Gupta A 2021 Marine Heatwaves *Ann. Rev. Mar. Sci.* **13** 313–42
Pedlosky J 1987 *Geophysical Fluid Dynamics* vol 710 (Springer)
Peng Q, Xie S P, Wang D, Huang R X, Chen G, Shu Y, Shi J R and Liu W 2022 Surface warming–induced global acceleration of upper ocean currents *Sci. Adv.* **8** 1–13
Qiu B and Lukas R 1996 Seasonal and interannual variability of the North Equatorial Current, the Mindanao Current, and the Kuroshio along the Pacific western boundary *J. Geophys. Res. Ocean* **101** 12315–30
Sasaki Y N and Umeda C 2021 Rapid warming of sea surface temperature along the kuroshio and the china coast in the East China sea during the twentieth century *J. Clim.* **34** 4803–15
Sen Gupta A, Stellema A, Pontes G M, Taschetto A S, Vergés A and Rossi V 2021 Future changes to the upper ocean Western boundary currents across two generations of climate models *Sci. Rep.* **11** 9538
Stommel H 1948 The westward intensification of wind-driven ocean currents *Trans. Am. Geophys. Union* **29** 202
Storer B A, Buzzicotti M, Khatri H, Griffies S M and Aluie H 2022 Global energy spectrum of the general oceanic circulation *Nat. Commun.* **13** 5314
Sun C *et al* 2022 Ecological forecasting and operational information systems support sustainable Ocean management *Forecasting* **4** 1051–79
Sverdrup H U 1947 Wind-driven currents in a Baroclinic Ocean; with application to the equatorial currents of the Eastern Pacific *Proc. Natl Acad. Sci.* **33** 318–26
Wang F *et al* 2023 The seas around China in a warming climate *Nat. Rev. Earth Environ.* **4** 535–51
Wang Q and Tang Y 2022 The interannual variability of Eddy Kinetic energy in the Kuroshio large meander region and its relationship to the Kuroshio latitudinal position at 140°E *J. Geophys. Res. Ocean* **127** 1–14
Wang Y-L, Wu C-R and Chao S-Y 2016 Warming and weakening trends of the Kuroshio during 1993–2013 *Geophys. Res. Lett.* **43** 9200–7
Wang Y and Wu C 2022 Rapid surface warming of the Pacific Asian Marginal Seas since the late 1990s *J. Geophys. Res. Ocean* **127** e2022JC018744
Wei Y, Huang D and Zhu X H 2013 Interannual to decadal variability of the Kuroshio Current in the East China Sea from 1955 to 2010 as indicated by *in-situ* hydrographic data *J. Oceanogr.* **69** 571–89
Wu C-R, Wang Y-L and Chao S-Y 2019 Disassociation of the Kuroshio Current with the Pacific Decadal oscillation since 1999 *Remote Sens.* **11** 276
Wu L *et al* 2012 Enhanced warming over the global subtropical western boundary currents *Nat. Clim. Change* **2** 161–6
Yang D, Yin B, Chai F, Feng X, Xue H, Gao G and Yu F 2018 The onshore intrusion of Kuroshio subsurface water from February to July and a mechanism for the intrusion variation *Prog. Oceanogr.* **167** 97–115
Yang D, Yin B, Liu Z and Feng X 2011 Numerical study of the ocean circulation on the East China Sea shelf and a Kuroshio bottom branch northeast of Taiwan in summer *J. Geophys. Res. Ocean* **116**
Yang H, Lohmann G, Krebs-Kanzow U, Ionita M, Shi X, Sidorenko D, Gong X, Chen X and Gowan E J 2020 Poleward shift of the major Ocean gyres detected in a warming climate *Geophys. Res. Lett.* **47** e2019GL085868
Young W R and Rhines P B 1982 A theory of the wind-driven circulation II. Gyres with western boundary layers *J. Mar. Res.* **40** 849–72 (available at: www.semanticscholar.org/paper/A-theory-of-the-wind-driven-circulation-II.-Gyres-oung-Peter/7326bd6fcb493ed10edecee5a950df8cc7afb004)
Zhu X, Nakamura H, Dong M, Nishina A and Yamashiro T 2017 Tidal currents and Kuroshio transport variations in the Tokara Strait estimated from ferryboat ADCP data *J. Geophys. Res. Ocean* **122** 2120–42